Behavioral Models for the Cosimulation and Optimization of Active Electronically Scanned Arrays

Charlotte Deville, Silvia Hernandez Rodriguez, Cyrille Menudier, Marc Thevenot, Benoit Lesur, Wissam Saabe, Christophe Mazière, Tony Gasseling

Behavioral Models for the Cosimulation and Optimization of Active Electronically Scanned Arrays

C. Deville[1], S. Hernandez Rodriguez[2], C. Menudier[2], M. Thevenot[2], B. Lesur[1], W. Saabe[3], C. Maziere[3], T. Gasseling[3]
[1] Safran Data Systems, La Teste-de-Buch, France, charlotte.deville@safrangroup.com
[2] XLIM – University of Limoges, Limoges, France, cyrille.menudier@xlim.fr
[3] AMCAD Engineering, Limoges, France, saabe@amcad-engineering.fr

***Abstract*—Active Electronically Scanned Arrays are versatile antenna solutions when high reconfiguration capabilities are required. However, they remain difficult to optimize due to their important degrees of freedom and their nonlinear components, sensitive to antenna impedance variation. This contribution describes the use of behavioral models for both nonlinear components and antenna radiating elements, allowing large array cosimulation and opening paths to several optimizations.**

***Index Terms*—phased arrays, behavioral models, amplifiers, active reflection coefficients, load-pull effect.**

I. Introduction

New markets for telecommunications are more and more dealing with reconfigurable directive antennas, with wide-angle beam scanning properties. It is especially true in the context of Low Earth Orbit (LEO) constellations where these antennas can be used for both the satellite payload and ground terminals [1]. Among the beam scanning architectures, active electronically scanned arrays (AESA) offer a great versatility, with individual control of amplitudes and phases. Even if their cost is important, recent advances on beamformer RF Integrated Circuits (RFIC) with Silicon technology propose a new technico-economical tradeoff [2]-[3]. Companies like Anokiwaves, Analog Devices or Renesas are now providing Commercial off-the-shelf (COTS) beamformers in Ku or Ka band with 4 to 16 channels [4].

However, they remain complex architectures and their optimization is a complex task. They especially combine RFIC with nonlinear devices (amplifiers) and quantized phase shifters. For the radiating panel, due to the wide-angle beam scanning requirements over the frequency range, the radiating elements input ports can present important active impedance variations. It represents a difficulty when they are connected to the amplifiers. It can significantly alter the power added efficiency (PAE) of the power amplifiers (PAs), resulting in difficulties to maintain a specified Effective Isotropic Radiated Power (EIRP) for the mission. Due to the moderate efficiency of Silicon PAs compared to other technologies like GaN, it is mandatory to optimize the active impedance of the antenna panel while the beam is steered. Even in this case, it is also important to accurately estimate the performance of the AESA during the design steps, instead of improving the design by iterative prototyping (too expensive and too long). To this end, behavior models can present significant advantages for the design of AESA, for both analysis and optimization.

In this contribution, a workflow with behavioral models for all the AESA element is presented, with an example of application in S-band. A preliminary EIRP optimization is proposed. The originality is based on the definition of the radiating panel behavioral model and its combination to nonlinear models for analysis.

II. Behavior Model Definition and Proposed Cosimulation Workflow

A. Behavioral model for nonlinear circuits

The power amplifier (PA) will influence the quality of the transmitted signal because of its high power and nonlinear behavior. As a source of harmonic distortion, multiple efforts have been devoted to the behavioral modeling of the PA trying to predict accurately its response [5]-[7]. A behavioral model is based on the identification of the nonlinear dynamics of the PA at the observation ports. It can be obtained from measurements or simulations data and it represents a trade-off between accuracy and simulation time [5]. It is especially faster than Harmonic-Balance simulations with a satisfactory accuracy provided the user respects the model domain of validity (based on VSWR and input power typically). Other blocks of the TX/RX chain as the low-noise amplifier (LNA) or the mixer may require a nonlinear modeling if they are driven to operate close to saturation [7]. Therefore, as the signals become more complex to meet the requirements of the new generations of wireless communications, accurate behavioral models are more and more necessary to predict the response of the radio chain at the design stage, especially in the design of large phased arrays with distributed amplifiers. Commercial softwares like AMCAD VSION offer these possibilities [8]. However, it can be difficult to link this kind of softwares to antenna accurate modeling tools.

B. Behavioral model for the radiating panel

Full-wave modeling of a radiating panel is a challenging task, especially with multilayer substrates with metallic via holes and hundreds of elements. Even if an analysis can be considered with High Performance Computing (HPC) and

GPU capabilities, a cosimulation with nonlinear circuits is not efficient and optimization steps is difficult to consider.
An interesting alternative is to consider a behavioral model of the radiating panel. To be exhaustive, this one should consider:

- The dispersion of the Active Reflection Coefficient (ARC) for the beam scanning directions $\{\theta_0, \varphi_0\}$ over the frequency range.

- The finiteness of the array, especially to evaluate the ARC, depending on the location of each radiating element.

- The active element pattern (AEP) of the array.

For the latter, it remains an approximation, as defined by Pozar, but it can be satisfactory, especially while one of the main challenges is more on the impact of scanned active impedance on each amplifier performance.

The behavioral model is then defined based on previous work of the laboratory [9]-[10]. It consists in defining an "identity card" of a unit cell with periodic boundaries, with the ARC computed for each $\{\theta_0, \varphi_0, \omega_0\}$ condition. It can be done with classical EM software, e. g. CST MWS, HFSS, within a small computation domain. Then, the equations in [10] are used to calculate the finite size scattering matrix of the array, from which the ARC of each radiating cell in the finite size panel can be deduced.

Therefore, it is then possible to consider the load-pull effect on the amplifier of an AESA when the PA is loaded by the active impedance of each antenna input port. This combination is more accurate compared to the infinite array approach where each antenna port active impedance is considered identical to its neighbors for a given $\{\theta_0, \varphi_0, \omega_0\}$ condition.

C. Proposed cosimulation workflow

The proposed workflow combining AMCAD VISION with its behavior models of PAs is illustrated in Fig. 1. The bilateral effect on a PA is considered and predicts its behavior under different load and source impedances. The load impedances correspond to the ones estimated by the behavioral model of the antenna panel aforementioned.

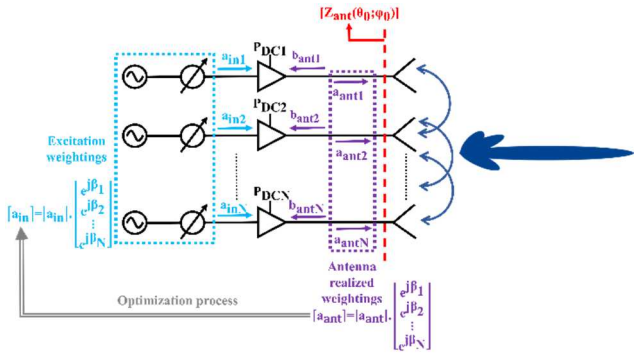

Fig. 1. Workflow basic summary – the dashed red line corresponds to the active reflection coefficients interface of the antenna panel connected to the behavioral model of the PAs. The analysis considers the bilateral effect on the amplifiers and allows tuning the antenna excitation weightings $[a_{ant,i}]$ under load-pull condition of PAs.

III. Example of an S-band AESA

This section presents a test case with the cosimulation of a 228-element AESA associated with Doherty power amplifiers.

A. Description of the AESA

The defined AESA scenario considers a S-band AESA working around 3.6 GHz, associated with Doherty-type amplifiers. This architecture of PA is chosen due to its quite stable Power Added Efficiency (PAE) for different input powers. The chosen model offers a 46% PAE on a 50 ohms impedance for a 16 dBm input power P_{in} (compression point) and 38% PAE for P_{in}=10 dBm. The behavioral model has been extracted from load-pull measurement facility of AMCAD Engineering until a VSWR equals to 3 and an input power swept from -30 dBm to 20 dBm, between 3.4 and 3.8 GHz. It means that the behavioral model should be used within these intervals. The dispersion of the amplifier gain and PAE under load-pull conditions is plotted in Fig. 2.

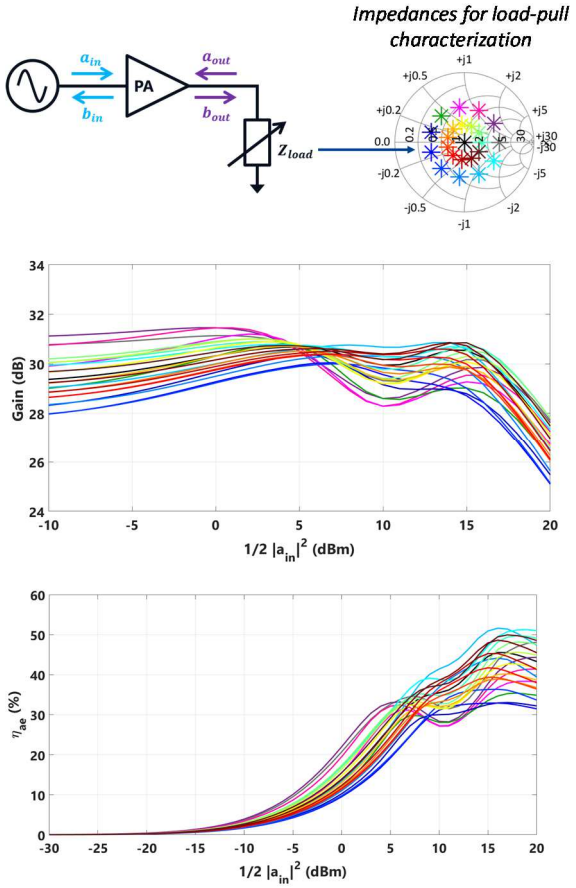

Fig. 2. Values of the amplifier gain under load-pull condition (different values of the load impedance) for different input powers at 3.6 GHz (middle) and PAE in the same conditions (bottom). Each color corresponds to the one on the Smith chart.

The antenna array part is also based on a previously measured radiating cell [9]. The radiating cell is optimized to satisfy a maximum active reflection coefficient (ARC) of -10 dB for each port, over the 3.4 - 3.8 GHz frequency band. The

behavioral model is based on the method described in part II.B and it has been previously validated in [9]. Here the behavioral model has been used to build the 228-element array in Fig. 3. This Figure illustrates the cells' location and their corresponding ARC for the on-axis radiation direction $\{\theta_0=0°;\varphi_0=0°\}$at 3.6 GHz. This result shows that this array does not suffer from ARC deterioration at this point.

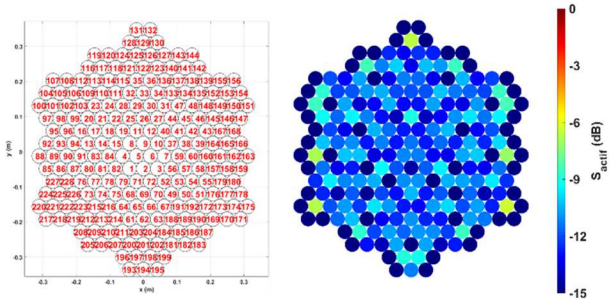

Fig. 3. Display of the cell's location in the array (Left) and map of active reflection coefficients for $\{\theta_0=0°;\varphi_0=0°\}$ direction at 3.6 GHz (Right) – Panel only (no amplifiers).

B. *Study of the AESA for wide-angle beam scanning and performance evaluation*

First, the EIRP level is set to 55 dBW for any angular direction between $\theta_0=0°$ and $\theta_0=60°$ over the frequency range. In this way, it will be possible to draw conclusions about the performance system for wide-angle beam steering. EIRP is a critical factor for SATCOM applications, due to the compliance with standards in order to avoid interferences. The expected weightings are calculated to apply a uniform weighting in amplitude across all the panel's ports, to avoid dispersion of the Power Added Efficiency (PAE) of the PAs. The working frequency is set at 3.6 GHz.

1) *Performances of the 228-element active array*

In this scenario, the objective is to set an EIRP of 55 dBW for any angular direction between $\theta_0=0°$ and $\theta_0=60°$ over the frequency range. Setting the EIRP level is a typical constraint for SATCOM applications. Here, the objective is to set the input power of the different amplifiers and to analyze the impact of the antenna active impedances on the PA performances. Fig. 4 shows the distribution of the 228 active impedances presented by the ports of the radiating panel, for the two directions aforementioned. This representation shows the impact of interactions between antenna ports and amplifiers on each active impedance. Indeed, the points corresponding to the location of active impedances on the Smith chart are more dispersive for the $\{\theta_0=0°;\varphi_0=60°\}$direction (Fig. 4. b)) than in the $\{\theta_0=0°;\varphi_0=0°\}$ direction, as can be expected. Notice that the active impedances are the load impedances of the amplifiers. The beam steering affects the performance of all amplifiers and, consequently, the overall performance of the system. This result is expected, but in this calculation, it is possible to extract each contributor and to quantify the effects on each channel. It is helpful to anticipate thermal dissipation or further optimization.

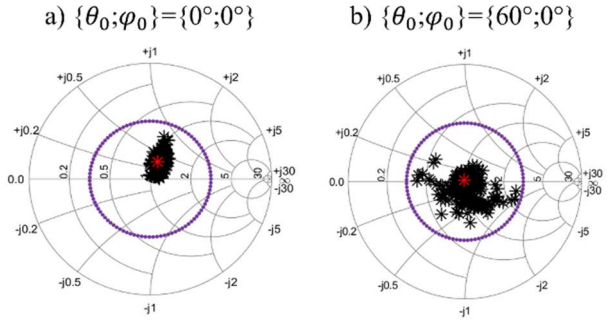

Fig. 4. Distributions of the 228 active impedances of the radiating panel, connected to their corresponding amplifiers. In purple : circle delimiting the validity of the amplifier model

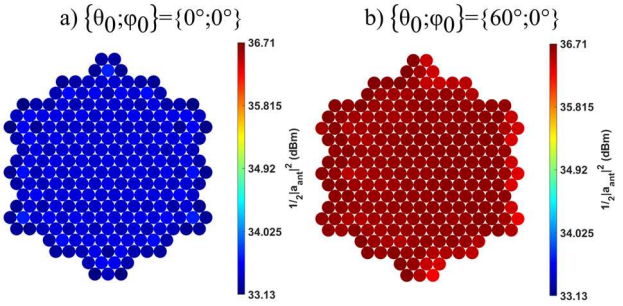

Fig. 5. Maps of the amplitude of antenna-realized weightings (dBm) for $\{\theta_0=0°;\varphi_0=0°\}$ and $\{\theta_0=60°;\varphi_0=0°\}$ directions

Then, the antenna realized weightings are represented in Fig. 5 for the directions $\{\theta_0=0°;\varphi_0=0°\}$ and $\{\theta_0=60°;\varphi_0=0°\}$. It describes the power level required at the antenna inputs to reach a 55 dBW EIRP in the steering direction. The power level required is higher in the direction $\{\theta_0=60°;\varphi_0=0°\}$, due to the need to compensate for gain loss caused by the beam steering. Moreover, the map of the antenna realized weightings allow showing that they are relatively uniform for the both directions. It is mainly due to the good matching of the radiating elements observed in Fig. 3, and their slight degradation for $\{\theta_0=60°;\varphi_0=0°\}$.

Then, Fig. 6 and Fig. 7 present the energy efficiency of the 228-element active array. Fig. 6 illustrates the DC consumption of each amplifier when all the amplifiers are connected to their respective ports, for both directions. The DC consumption is relatively uniform in the $\{\theta_0=0°;\varphi_0=0°\}$ direction with a mean level of 9.5 W. The map corresponding to the $\{\theta_0=60°;\varphi_0=0°\}$ direction presents variations of consumption between each amplifier, due to the important beam steering and all the interactions between antenna ports and amplifiers. Thanks to the proposed cosimulation workflow, these results allow to quantify the perturbations, which affect the performances like consumption. It is then possible to anticipate correction in the design or better sizing of thermal dissipators and power supplies. Moreover, notice that the compensation of gain loss drives to an increase of

consumption to maintain an EIRP level of 55 dBW in the $\{\theta_0=60°;\varphi_0=0°\}$ direction.

Fig. 7 shows the power-added efficiency (PAE) obtained for each amplifier in the radiation scenario defined above. In the $\{\theta_0=0°;\varphi_0=0°\}$ direction, PAE is relatively uniform across all amplifiers, and the level is around 22%. As well as for the consumption, the direction $\{\theta_0=60°;\varphi_0=0°\}$ leads to higher disturbances of PAE for all amplifiers (Fig. 7. b)). Furthermore, the PAE of each amplifier tends to increase in the $\{\theta_0=60°;\varphi_0=0°\}$ direction. This describes a better use of amplifiers power in this context, where the same level of EIRP must be provided whatever the pointing direction. Next, some amplifiers in the active array stand out from the others in the $\{\theta_0=60°;\varphi_0=0°\}$ direction. Indeed, the amplifiers located on the right of the panel, in the direction where the beam is steered, present a higher DC consumption (Fig. 6. b) and a lower power-added efficiency (Fig. 7. b)

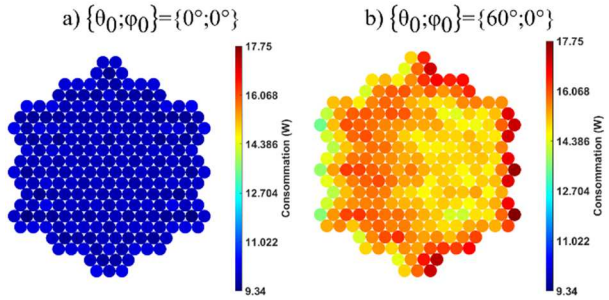

Fig. 6. Maps of PA DC power consumption (W) for $\{\theta_0=0°;\varphi_0=0°\}$ and $\{\theta_0=60°;\varphi_0=0°\}$ directions.

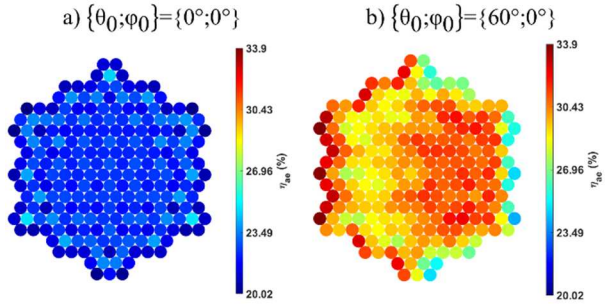

Fig. 7. Maps of the power-added efficiency (%) for $\{\theta_0=0°;\varphi_0=0°\}$ and $\{\theta_0=60°;\varphi_0=0°\}$ directions.

Regardless of the beam steering, the proposed analysis allows to the EIRP level at the value set in the radiation scenario. To this end, the appropriate excitation weightings are set at the input of the amplifiers in order to theoretically provide the necessary power level at the radiating panel, and thus the expected EIRP level. In this particular case, the radiating elements and amplifiers are chosen and then analyzed. However, this kind of simulation can run in a few minutes and it can be associated in the future to more complex optimizations under constraints, especially to be compliant with a given overall efficiency, side lobe level, power consumption restriction, etc…

CONCLUSION

This work has shown the possibility to define a cosimulation workflow of AESA based on behavioral models for all the components. The originality is mainly due to the antenna panel behavioral model, considering the finiteness of the structure. It is then possible to compute the efficiency of the whole antenna and also the one of each channel, with the amplifiers and the radiating elements. It is helpful at an early stage of the design of an AESA or to optimize an EIRP level. It is also open to further optimization process in the future.

ACKNOWLEDGMENT

This work is associated with the joint laboratory X-SELANS (Xlim-Safran Electronics Lab for ANtennaS), in the context of the French National Research Agency program ANR-19-LCV2-0008. The authors want to thank AMCAD Engineering for their continuous support and for providing the last features of their AMCAD VISION software.

REFERENCES

[1] G. Amendola et al., « Low-Earth Orbit User Segment in the Ku and Ka-Band: An Overview of Antennas and RF Front-End Technologies », IEEE Microwave, vol. 24, nº 2, p. 32-48, févr. 2023, doi: 10.1109/MMM.2022.3217961.

[2] B. Sadhu, X. Gu and A. Valdes-Garcia, "The More (Antennas), the Merrier: A Survey of Silicon-Based mm-Wave Phased Arrays Using Multi-IC Scaling," in *IEEE Microwave Magazine*, vol. 20, no. 12, pp. 32-50, Dec. 2019, doi: 10.1109/MMM.2019.2941632.

[3] O. Kazan, Z. Hu, A. Alhamed and G. M. Rebeiz, "A Wideband X/Ku/Ka-band SATCOM 8-Channel SiGe Transmit Beamformer Chip in a 16-Element Phased-Array," *2023 17th European Conference on Antennas and Propagation (EuCAP)*, Florence, Italy, 2023, pp. 1-3, doi: 10.23919/EuCAP57121.2023.10133001.

[4] https://www.analog.com/en/products/adar3000.html

[5] J. C. Pedro and S. A. Maas, "A comparative overview of microwave and wireless power-amplifier behavioral modeling approaches," in *IEEE Transactions on Microwave Theory and Techniques*, vol. 53, no. 4, pp. 1150-1163, April 2005.

[6] A. Zhu and T. J. Brazil, "An Overview of Volterra Series Based Behavioral Modeling of RF/Microwave Power Amplifiers," *2006 IEEE Annual Wireless and Microwave Technology Conference*, Clearwater Beach, FL, USA, 2006, pp. 1-5.

[7] E. Ngoya and S. Mons, "Progress for Behavioral Challenges: A Summary of Time-domain Behavioral Modeling of RF and Microwave Subsystems," in *IEEE Microwave Magazine*, vol. 15, no. 6, pp. 91-105, Sept.-Oct. 2014.

[8] https://www.amcad-engineering.com/software/vision/

[9] R. Lamey, M. Thevenot, C. Menudier, E. Arnaud, O. Maas and F. Fezai, "Interleaved Parasitic Arrays Antenna (IPAA) for Active VSWR Mitigation in Large Phased Array Antennas With Wide-Angle Scanning Capacities," in IEEE Access, vol. 9, pp. 121015-121030, 2021, doi: 10.1109/ACCESS.2021.3108231.

[10] B. Lesur, A. Maati, M. Thevenot, C. Menudier, E. Arnaud, T. Monediere, C. Melle, D. Chaimbault, A. Karas, "A Large Antenna Array for Ka-band Satcom-on-the-Move Applications - Accurate Modelling and Experimental Characterization", IEEE Transaction on Antennas and Propagation. vol. 66, no. 9, pp. 4586-4595, Sept. 2018. doi: 10.1109/TAP.2018.2851296.